MARITIME TRANSPORTATION RESEARCH AND EDUCATION CENTER
TIER 1 UNIVERSITY TRANSPORTATION CENTER
U.S. DEPARTMENT OF TRANSPORTATION

Towards integrating resilience into everyday transportation practices of coastal and river valley communities

07/10/2018 – 03/31/2021

Nelida Herrera, Ph.D.
nherre2@lsu.edu
Louisiana State University

Brian Wolshon, Ph.D., P.E., P.T.O.E. (PI)
brian@rsip.lsu.edu
Louisiana State University

Mohammad Shapouri, Ph.D.
mshapo1@lsu.edu
Louisiana State University

Siavash Shoojat, Ph.D.
Ssshoja1@lsu.edu
Louisiana State University

March 31st, 2021
FINAL RESEARCH REPORT
Prepared for:
Maritime Transportation Research and Education Center

University of Arkansas
4190 Bell Engineering Center
Fayetteville, AR 72701
479-575-6021

Acknowledgements
This material is based upon work supported by the U.S. Department of Transportation under Grant Award Number 69A3551747130. The work was conducted through the Maritime Transportation Research and Education Center at the University of Arkansas.

Abstract

Coastal and river valley communities have become increasingly vulnerable to sea level rise and other disasters which can disrupt transportation systems. Therefore, it is important for these systems to be resilient. Analyzing the resilience of transportation systems is important for practitioners and decision makers to identify weaknesses within the network and analyze design alternatives that can improve resilience. Even though research has been conducted in the area of resilience, integrating this concept into everyday transportation practices to prepare for disasters and other disruptions (e.g. inclement weather, traffic incidents, road blockages) remains a challenge.

The goal of this research was to advance the state-of-the-art in transportation activities to integrate resilience into traffic analyses to assist coastal and river valley communities in their resilience practices. This study demonstrated the use of resilience methods and metrics in the analysis of a crash which blocked a segment of a coastal freeway modeled using microscopic traffic simulation. The study demonstrated the use of resilience metrics and methods which advances the next steps for future research to develop new or enhanced tools and methods that can be transferred to coastal and river valley communities for their resilience practices.

1. Introduction

Improving resilience of transportation systems has been emphasized by The U.S. Department of Transportation (USDOT) in the Moving Ahead for Progress in the 21st Century (MAP-21) Act (FHWA, 2017). A resilient system has the ability to withstand, respond to, and recover rapidly from disruptions (FHWA, 2015). This is important to minimize losses and recover functionality when a disruption occurs. Therefore, integrating resilience analyses in the planning, management, and operations of transportation systems is important to improve the resilience of transportation systems.

Resilience analyses can be performed to identify network weaknesses and quantify the ability of transportation systems to absorb and recover from disruptions. Disruptions can be related not only to disasters or other major events but also weather and road events (e.g. traffic incidents) that impact traffic performance on a daily basis.

More research on resilience is emerging which is promising to close the gaps in knowledge regarding the methods and metrics that can be used to quantify resilience in transportation projects. However, integrating this concept into everyday transportation practices to prepare for these disasters and other disruptions remains a challenge. Therefore, this research aimed at integrating resilience into traffic analyses to assist coastal and river valley communities in their resilience practices. Resilience methods and metrics available in the literature were assessed and some of these were selected to demonstrate their use in a typical alternative analysis study. To do this, this research used microscopic traffic simulator Vissim to model a disruption caused by a vehicular crash which resulted in a lane blockage along a segment of Interstate 5 in San Diego, California. Crash scenarios with active and inactive ramp metering were assessed to measure the resilience of the system under each condition.

A review of the literature related to the definition of resilience and resilience methods and metrics was conducted and summarized in section 2 of this report. The methodology of this study is presented in section 3. It describes the simulation network and the calibration of the simulation model. A description of the scenarios analyzed is also provided. The results section presents and discusses the measures used and the findings of the analysis conducted. Finally, the conclusion section summarizes the findings and contributions of the study as well as study limitations and future research.

2. Research Background

In this section, the general concept of resilience is summarized as it relates to transportation and other disciplines and fields. Then, a description of methods and metrics implemented in previous research studies is provided.

2.1 Definition of Resilience

Holling (1973) initially defined resilience focused on stability of ecological systems. Subsequently, researchers integrated resilience in different fields including economics (Vugrin et al., 2010), urban structure (Attoh-Okine et al., 2009), business management (McManus et al., 2008; Somers, 2009), computer science (Najjar & Gaudiot, 1990; Trivedi et al., 2009), supply-

chain management (Chen and Miller-Hooks, 2012; Cox et al. 2011), and engineering (Blackmore & Plant, 2008; Murray-Tuite, 2006).

In the context of traffic and transportation systems, resilience has gained more attention since 2011 specifically from the wake of natural disasters (Balal et al., 2019). The Federal Highway Administration (FHWA) defines resiliency as "the ability to prepare for changing conditions and withstand, respond to, and recover rapidly from disruptions" (FHWA, 2015).

Currently, there is no widely accepted definition of resilience in the literature because it is highly related to network/infrastructure type and study objectives (Bozza et al., 2017). Some research has indicated that resilience overlaps with other concepts including vulnerability and robustness. Robustness is related to the ability of the system to maintain the original functionality level, while vulnerability describes the susceptibility of the system to extreme events and performance loss (Berdica, 2002; Reggiani et al., 2015). Resilience involves resistance to disturbances as well as the ability to recover from disturbances (Calvert and Maaike, 2017). A system that fails but recovers quickly can be considered resilient but not robust because it was not able to maintain the original functionality level (Calvert and Maaike, 2017).

Bruneau & Reinhorn (2007) defined resilience for physical systems including transportation infrastructure through the following dimensions:

- Robustness: Strength of a system or elements of a system to withstand extra demand and maintain original functionality level.
- Redundancy: Existence of alternate elements of systems, systems or unit of analysis which meet external demand under stress.
- Resourcefulness: The capacity to determine the problems and mobilize required resource and service during disruption.
- Rapidity: The speed at which a system regains a level of functionality and service.

For transportation networks, Murray-Tuite (2006) indicated ten dimensions of a resilient transportation system: redundancy, diversity, efficiency, autonomous components, strength, adaptability, collaboration, mobility, safety, and the ability to recover quickly. Resilience was defined as a characteristic that indicates system performance under unusual conditions, recovery speed, and the amount of outside assistance required to restore the system to its original functional state. According to Nicholson et al., (2016) vulnerability and recoverability are the primary dimensions of resilience.

2.2 Resilience Measures

Researchers have investigated different approaches to measure resilience of transportation systems by quantifying system performance before, during, and after a disruptive event. Figure 1 illustrates a typical system performance over time after a disruptive event. In the figure, the disruptive event causes performance Q to drop at t_0. Thereafter, the system starts to recover and restore to its initial performance at $t_0 + t_r$ forming a triangular area which is referred to as ''resilience triangle" (Bruneau et al., 2003). The height of the triangle is the magnitude of the disruption measured as performance loss while the base of the triangle is the time it takes to

recover. Lastly, the area of the triangle captures the overall resilience. Bruneau & Reinhorn (2007) mathematically defined resilience as follows:

$$R = \int_{t_0}^{t_1} [100 - Q_t]\, dt \tag{1}$$

Where:

Q_t is the quality of the infrastructure over time
t_0 and t_1 are disturbance occurrence and system recovery times, respectively.

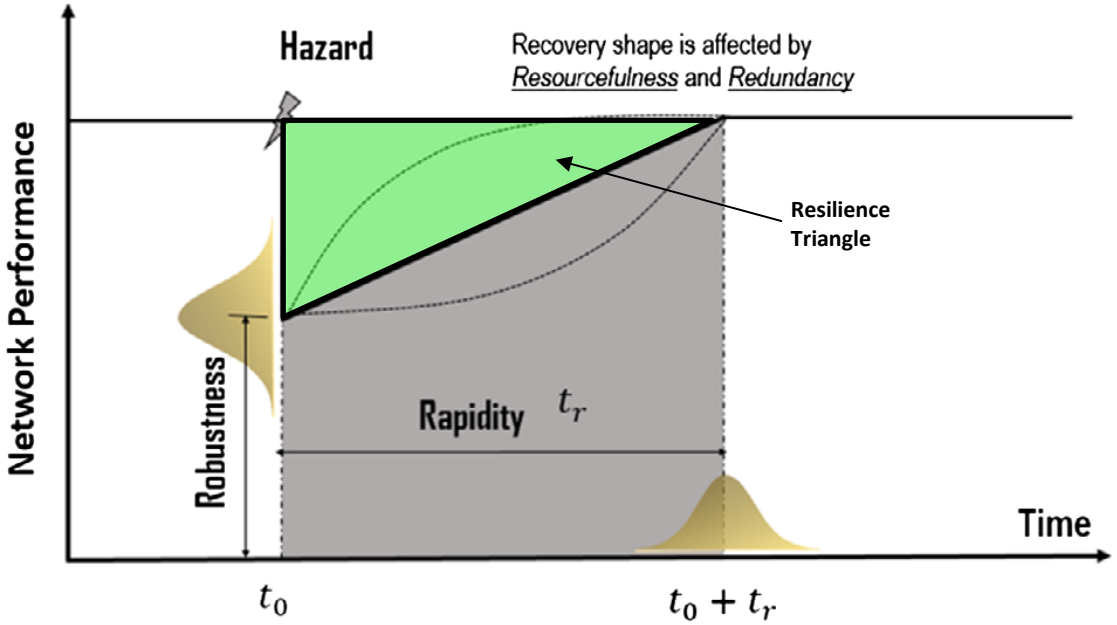

Figure 1 Resilience curve (Adapted from Zhang & Wang, 2016)

This equation assumes that the original state of the system is constant at 100 percent functionality. While that can be case for a static physical structure, for a complex and dynamic systems such as a roadway networks, the original state without the disruption may not be constant (Balal et al., 2019). For example, consider a freeway network before, during, and after the peak period where the flow of vehicles is not constant because of the variation in demand. This demand fluctuation can activate bottlenecks and cause loss in functionality temporarily. If a disruption (e.g. road blockage from a crash) is introduced, then the loss in functionality during and after the crash should be compared to the systems performance without the disruption at its "normal" performance for the same period. Hence it is more appropriate to consider the un-disrupted performance of a system as a function of time and not as a constant. In addition, this equation assumes the loss in functionality happens immediately, however, the loss could be more gradual and hence the slope of the loss would be less than 1. The slope will be a function of robustness and adaptability. Once the maximum loss occurs, the recovery process starts. All

of these stages add to the resilience (Balal et al., 2019). Therefore, resilience was proposed to be measured by Balal et al., 2019 as follows:

$$R = \int_{t_0}^{t_1} \left[S_t - S_{o(t)} \right] dt \tag{2}$$

Where:

S(t) is the system performance over time t,
S_0 is the normal steady state systems performance
t_0 and t_1 are times at the initial state and at the recovered state, respectively.

Bozza et al. (2017) proposed the following resilience measure which is scaled to [0, 1]:

$$R_2 = \frac{\int_{t_0}^{t_1} S(t)dt}{\int_{t_0}^{t_1} S_0(t)dt} \tag{3}$$

Where:

S(t) is the system performance over time t,
S_0 is the normal steady state systems performance
t_0 and t_1 are times at the initial state and at the recovered state, respectively.

Typical measures used in the literature include volume, travel speeds, travel time, delay, capacity, and queue length. Figure 2(a) shows a disruptive event which occurs at t_0 and causes a sudden change in the state from S_0 to S_1 which results in an increase the measure (e.g. travel time). The same disruption causes a sudden decrease in a measure (e.g. traffic volumes) as shown in Figure 2(b). In some cases, the network deteriorates gradually rather than suddenly as illustrated in Figure 2(c) and Figure 2(d). In this case the network's operation deteriorates gradually from S_0 at t_0 to S_1 at t_2. At t_2, the system starts to recover, and restores its original state S_0 at t_1. A ''resilience trapezoid" can be observed as shown in Figure 2(e) and Figure 2(f) when the state of the network's operation reaches a performance S_1 and it stays constant for a period of time, before it starts its recovery (Booza et al., 2017; Balal et al., 2019).

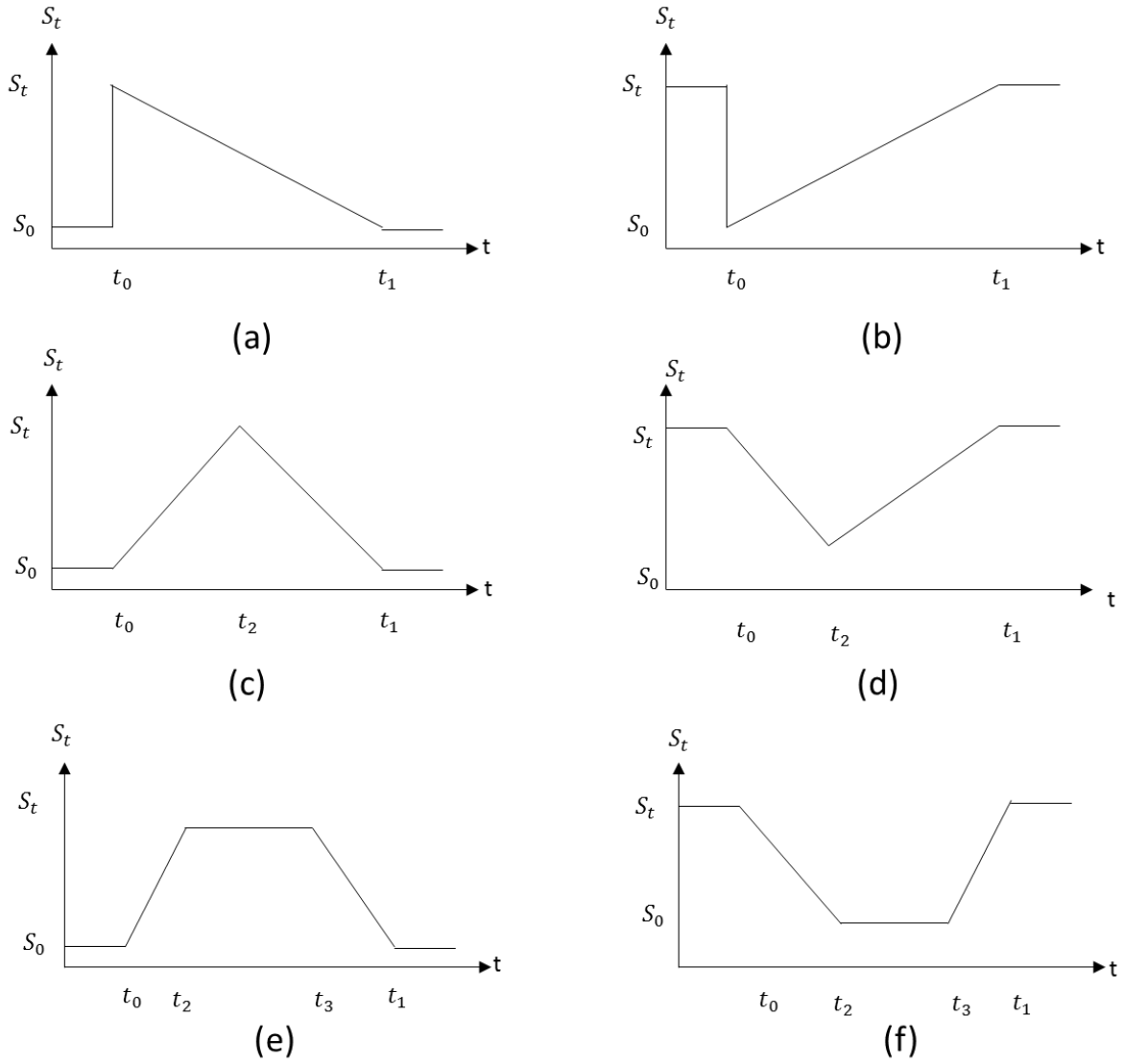

Figure 2 Resilience Curves (Adapted from Balal et al., 2019)

Other resilience methods were found in the literature. For example, Attoh-Okine et al. (2009) developed a resiliency index for urban infrastructure. Li and Lence (2007) used the ratio of the probability of failure and recovery as a measure to formulate a resiliency index for water resources systems. Henry and Ramirez-Marquez et al. (2012) introduced a time dependent method to measure resilience focused on the recovery process of disturbances. D'Lima and Medda (2015) developed a metric to quantify resilience based on the principles of mean-reversion considering the random nature of disruptions. The model accounted for event severity and expected rate of recovery for abrupt and slowly-occurring events. A case study was conducted based on disruptions of the underground service in London. Passenger counts were used as measures of service loss to assess the resilience of the affected underground lines and also the parallel lines that were indirectly impacted by the disruption. Zhu et al., (2016) calculated recovery curves based on the logistic function. The research used big data sets for taxi and transit

ridership to evaluate the resilience of New York's roadway and subway systems following hurricanes Sandy and Irene. Number of taxi trips and daily subway ridership were used as measures of service loss in the resiliency analysis. Farhadi et al. (2016) developed time-dependent resiliency plots showing time resiliency and port transit count resiliency based on two performance indicators: average vessel dwell time within the port areas of interest and net vessel transits into and out of the port areas of interest. This study was based on the work from Henry and Ramirez-Marquez et al. (2012). Donovan & Work (2017) used GPS data from taxis during adverse events to measure urban transportation system resilience. They computed normalized travel time per mile (pace) deviation between defined zones during unusual events to assess the impact of the disturbance on a network. Calvert & Snelder (2017) studied resilience of a road section in relation to the network based on traffic flow fluctuation, speed, and road capacity. The study developed a Link Performance Index for Resilience (LPIR) to evaluate the resilience level of individual road sections focusing on everyday operational traffic situations rather than just on disasters or major events. The LPIR includes a resistance (uncongested state) and a recovery (congested state) part that is quantified based on the index of density (*k*) over critical density (*kcrit*) shown in Equation 4 and can be re-written as show in Equation 5 (Calvert & Snelder, 2017).

$$k = \frac{k}{k_{crit}} \tag{4}$$

Where:

$\mathrm{k} = \text{density}$

k_{crit} = *critical density*

$$\text{LPIR} = \sum_{t=0}^{T} \left\{ \begin{array}{ll} \dfrac{\left[\dfrac{q+\psi^{q}}{v}\right]}{\left[\dfrac{q_{\text{cap}}(g,h)\cdot f+\psi^{\text{cap}}}{v_{\text{crit}}}\right]} & \text{for } k \le k_{\text{crit}} \\ \dfrac{\left[\dfrac{q+\Delta q}{v_{\text{eq}}(q)}\right]}{\left[\dfrac{q_{\text{cap}}(g,h)\cdot f-q_{\text{cd}}}{v_{\text{crit}}}\right]} & \text{for } k > k_{\text{crit}} \end{array} \right\} \Big/ T. \tag{5}$$

Where:

q = flow

v = speed

ψ^{q} = distance headway between consecutive vehicles (km)

v_{crit} = critical speed

v_{eq} = derived speed

$\mathrm{q}_{\mathrm{cap}}$ = road capacity

g = road characteristics

h = traffic characteristics

f = temporal capacity reductions (i.e. incidents)

k = density

k_{crit} = *critical density*

T = Time

The total LPIR score per road section is the average over all time intervals for the considered period (Calvert & Snelder, 2017). This metric can be used to quantify the relative resilience of a road section compared to other road sections (Calvert & Snelder, 2017). A value of LPIR less than or equal to 1 indicates that a road section is able to resist and/or recover promptly from a disruption. A segment with an LPIR larger than 1 is not always non-resilient (Calvert & Snelder, 2017). Normalization of the LPIR may be applied, as this may make comparison between values from different road sections easier (Calvert & Snelder, 2017). However this has the drawback that the quantitative interpretation of the index is lost (Calvert & Snelder, 2017).

Topological indices have also been evaluated as measures to capture the performance of a system and provide a fundamental understanding of network resilience (Crucitti et al., 2004; Gay & Sinha, 2013; Holme et al., 2002). Fundamentally, this method evaluates network topology and the effect of link/node removal on network connectivity and robustness/vulnerability (Calvert & Snelder, 2018; Gay & Sinha, 2013; Reggiani et al., 2015; Scott et al., 2006; Sullivan et al., 2010). While random link/node removal simulates the effect of a natural disaster or a vehicle crash, deliberate removal reflects intended attacks which cause maximum damage to the system (Gay & Sinha, 2013). Some research studies have implemented this concept. For example, Zhang & Wang, 2016 integrated network topology with average daily traffic (ADT) and reliability of network components to propose a quantitative resilience metric. Ip & Wang (2011) quantified resilience for each node as a weighted average number of reliable passageways to all other nodes. In the study, transportation network resiliency was considered as the sum of the resilience of all nodes in the network.

Complex network theory and simulation have also being used in resilience and robustness evaluations. For example, Murray-Tuite (2006) evaluated transportation resilience as a hypothetical evacuation scenario using the traffic simulation software DYNASMART-P. The study implemented two different traffic assignment methods: system optimum (SO) and user equilibrium (UE). Four dimensions of resilience (adaptability safety mobility and recovery) were considered in the study. Adaptability was measured as the percentage of vehicles seen at typical infrastructure (e.g. high occupancy lanes). Safety was measured as the number of traffic incidents that occurred along a given road. This information was obtained from the National Highway Traffic Safety administration (NHTSA). A second potentially relevant safety measure was the number of vehicles exposed to hazards. For example, the number of vehicles passing by lakes

and rivers prone to flooding. Mobility was measured based on the following: 1) evacuation time estimates; 2) the average travel time between zones and the standard deviation of response vehicles such as ambulances to quantify the ability of these to travel from one zone to another; 3) queue length evaluated at various thresholds; 4) amount of time that average speeds slower than a threshold were maintained; 5) volume to capacity ratios for each link. Recovery was measured by the amount of time, money, and outside assistance required to restore an acceptable level of service. This was measured as the amount of time required to alleviate congestion based on 1) time at which the queue length on link a returns to a predetermined range, 2) time at which the speed on the link returns to an or exceeds to the post speed limit, and 3) time at which the volume to capacity ratio for a link returns to a pre-specified range.

Balal et al., (2019) investigated the relation between five different performance measures: queue length, link speed, link travel time, frontage road delay, and detour route delay due to traffic incidents using traffic simulation. The results suggested that the five indicators are not statistically correlated, and each measurement leads to different outcomes.

Based on the review of the literature, there is still lack of consistency of resilience measures that can be implemented in transportation studies. For this study, travel speeds and travel times were selected as performance to measure resilience. In addition, the LIPR score developed by Calvert & Snelder (2017) was used. A network-level analysis was also conducted based on network performance measures: vehicle hours traveled (VHT) and vehicle hours of delay (VHD). Microscopic traffic simulator Vissim 8.00 was used in this study to collect these measures. The simulation modeled a lane closure due to a crash that blocked a segment of the freeway. The analysis included the implementation of an alternative to improve resilience and a typical “Do-Nothing” or “No-Build” alternative used in traffic studies. It is important to mention that more research is still needed to understand the resilience metrics that can be used in different type of scenarios so that guidance can be provided to practitioners.

3. Research Methodology

A 4.5- mile segment of Interstate 5 in San Diego, California was modeled in this study using Vissim 8.0 to simulate different crash scenarios causing temporary lane blockages. The corridor extended from Manchester Avenue to Leucadia Boulevard and included four on-ramps and four off-ramps as shown in Figure 3. Aerial imagery was used to match roadway geometry and speed limits. The corridor included a distinct traffic bottleneck section that regularly becomes congested and, therefore, it ensures observations of congested and uncongested states. Traffic data at the mainline bottleneck section as well as all on- and off-ramp sections were collected. More specifically, traffic volume and speed data were collected in five-minute intervals from the PeMS website[1] for a single weekday (October 8th, 2015) and inputted into the Vissim model (PeMS, 2015). The freeway modeled traffic flowing northbound for a 24-hour period.

[1] http://pems.dot.ca.gov

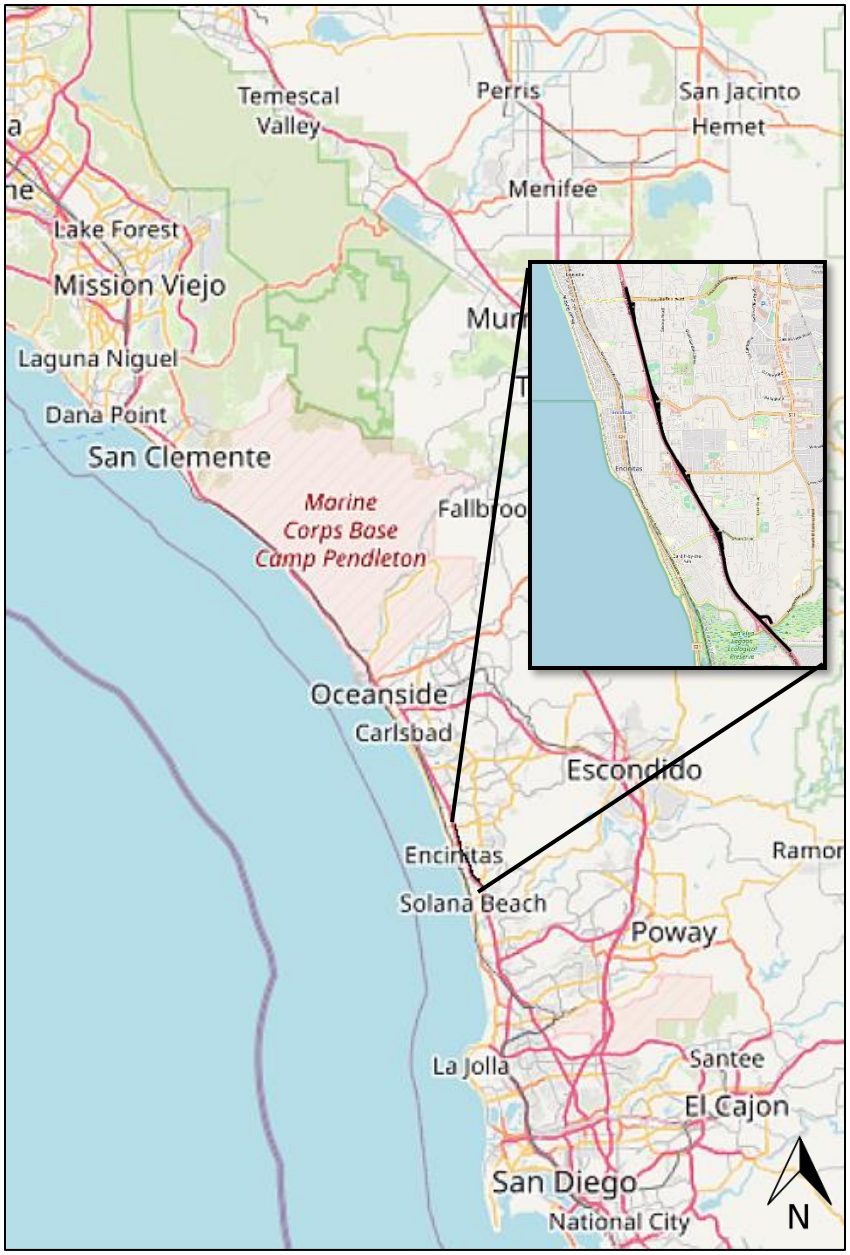

Figure 3 Simulated Road Network

3.1 Simulation Model Calibration

To simulate realistic traffic operations within the corridor, the VISSIM model was calibrated to replicate real-world speeds and volumes at the bottleneck section for the entire day (24 hours). Vissim COM programming was used to select different Vissim driving behavior and lane changing parameter values that minimized the differences between the observed and simulated speeds and volumes.

To calibrate traffic volumes, the GEH[2] statistic was used as a measure of effectiveness (MOE). The GEH statistic is a well-known empirical measure that is widely used in transportation studies to calibrate hourly traffic volumes (Dowling et al., 2004). Its formula is given in Equation 6.

$$GEH=\sqrt{\frac{2(m-c)^2}{m+c}} \tag{6}$$

Where:

m = output traffic volume from the simulation model (veh/h)

c = input traffic volume (veh/h)

It is important to note that the GEH formula can only be used for hourly volumes. Because calibrating the hourly volumes for the whole day was of interest in this study, the percentage of hourly volumes with an acceptable GEH value was regarded as an appropriate calibration target.

According to the FHWA (2004), the GEH statistic for individual link flows is acceptable only if GEH is less than 5 for a least 85 percent of the all cases (Dowling et al., 2004). This suggests that for an observation period with 24 different GEH values (i.e. one GEH for each hourly volume), at least 21 of GEH values should have a value less than 5.

The root mean squared percentage error (RMSPE) was used as an MOE to calibrate the speeds. The RMSPE is a measure that is usually applied to calculate the deviation of the simulation speeds from the observed speeds. Therefore, as a first step, the Van Aerde model was fitted to the real-world 5-minute observations.

The Van Aerde model is a continuous function that describes the speed-flow-density relationship based on a simple car following equation (Shojaat et al., 2018). To estimate the model parameters, reasonable starting values for the key traffic flow variables (i.e. capacity, free-flow speed, speed at capacity, and jam density) are assumed and a starting set of parameters (c_1, c_2, c_3, s_f) were calculated using Equation 7. Next, using a non-linear regression, an iterative approach was implemented to estimate the model parameters which minimize the sum of squared errors of the model.

$$d=\frac{1}{h}=\frac{1}{c_1+\frac{c_2}{s_f-s}+c_3.s} \tag{7}$$

where

d = density (veh/km)

h = distance headway between consecutive vehicles (km)

s_f = free flow speed (km/h)

[2] Named after its inventor Geoffrey E. Havers.

c_1 = fixed distance headway parameter (km)

c_2 = first variable headway parameter (km^2/h)

c_3 = second variable distance headway parameter (h^{-1})

s = speed (km/h)

Once the Van Aerde model is fitted to the observed field data and parameters of the model are calibrated, for every simulated volume, the difference between its simulated speed and the observed speed (i.e. the speed that is estimated for the simulated volume from the Van Aerde model) was measured and the RMSPE was calculated according to Equation 8. RMSPE of 5 percent is usually regarded as an appropriate calibration target for the speeds (Shojaat, 2017).

$$\text{RMSPE} = \sqrt{\frac{1}{N} \cdot \sum_{n=1}^{N} \left(\frac{x_n^{sim} - x_n^{obs}}{x_n^{obs}} \right)^2} \quad (8)$$

where

x_n^{sim} = n^{th} simulated speed (mph)

x_n^{obs} = n^{th} observed speed (mph)

To calibrate the speeds, the RMSPE was used as an appropriate MOE. Thus, the Van Aerde model was fitted to the real-world data and the differences between the simulated and the observed speeds were measured and used to calculate the RMSPE. It was observed that an RMSPE of 3.7 percent existed between the real and simulated speeds. Since this value was less than 5 percent, calibration accuracy was considered acceptable. Figure 4 shows the simulated and real-world speed-flow scatterplots for the mainline section of the corridor. Once the Vissim model was calibrated, the scenarios were created.

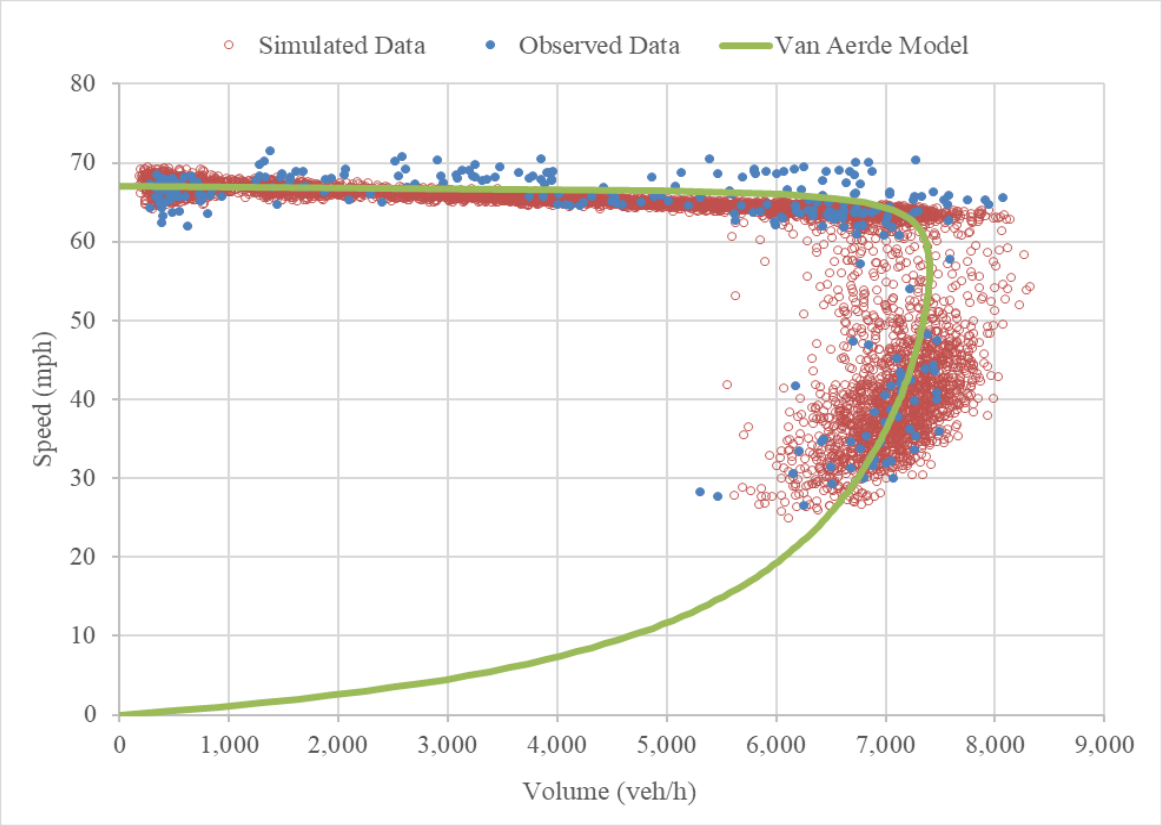

Figure 4 Comparison of Speed-Flow Scatterplots and the Van Aerde Model

3.2 Simulation Scenarios

To demonstrate the integration of resilience into traffic operation analyses for coastal and river valley communities to use in their resilience practices, a traffic disruption was modeled on the freeway. The disruption was caused by a hypothetical severe crash that blocked the right-most lane of a segment of the freeway. The lane blockage extended for less than 100 feet. Ramp metering was assessed as an operations strategy to measure resilience with and without this strategy. The freeway segment modeled in this study had signal heads for ramp metering. However, it was assumed for one of the scenarios that ramp metering was not functioning to assess the impact on the transportation system when a crash was present on the freeway. Ten simulations with different random seeds were run for each scenario. The scenarios evaluated are summarized below:

- Scenario 1: No Crash, No Ramp Metering
- Scenario 2: No Crash, Ramp Metering
- Scenario 3: Crash, No Ramp Metering
- Scenario 4: Crash, Ramp Metering

The first and second scenarios were the baselines which had no crash on the freeway. Therefore, the corridor operated without disruptions. In order to do a baseline comparison, the first scenario was modeled with the ramp meter inactive while the second scenario with the ramp

meter active. The third scenario modeled a crash on the freeway. The crash clearance time was assumed to be 60 minutes. Ramp metering was inactive in this scenario. This scenario could be considered the typical “Do-Nothing” alternative. The fourth scenario is similar to the third with a crash modeled on the freeway but ramp metering was active and considered as a traffic operations strategy.

3.3 Modeling the Crash in Vissim

An initial test was conducted to identify the location of the crash. For this test, a crash was modeled at three different locations along the freeway. The crash locations tested were selected based on changes in road geometry since this affects the impact on the system’s performance. The crash location with the highest impact was selected for the resilience analysis conducted in this study. It is important to mention that crash history is typically used to determine the location where crashes are more likely to occur. A vulnerability analysis to identify the critical links can also be conducted. However, the objective of this paper was to demonstrate a resilient-based analysis to assess the impacts of a crash under traffic operations strategies (i.e. ramp metering was considered in this study). Therefore, crash history was outside the scope of work for this project. However, the method presented in this study is still valid when that assessment is conducted.

Figure 5 shows the location of the crash selected for the analysis. The crash was modeled downstream of a freeway merge section. The crash simulation start and end times were 69,300 and 72,900 seconds, respectively.

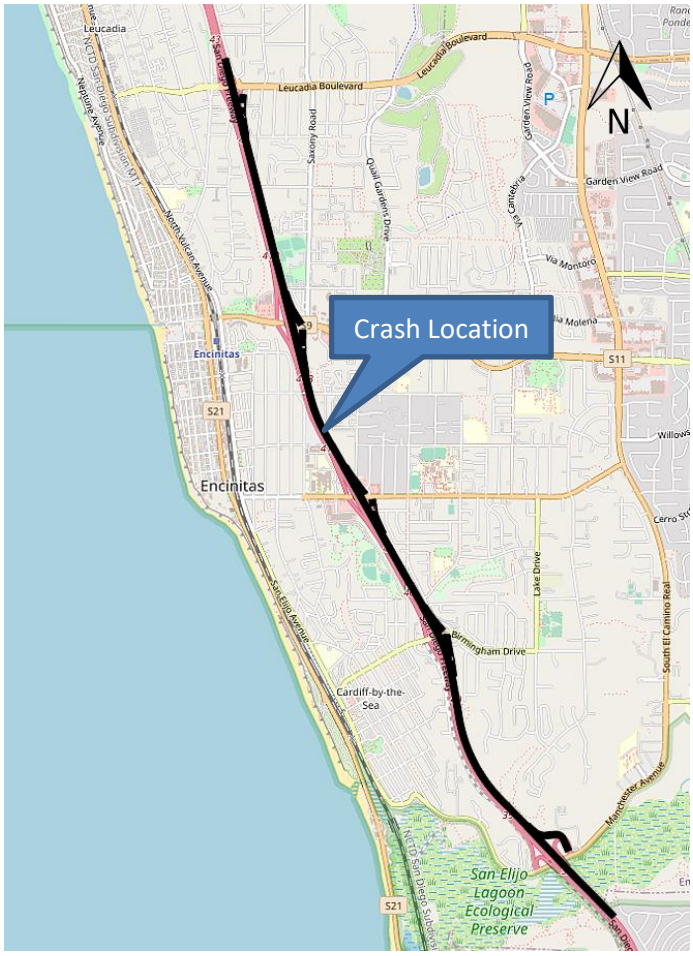

Figure 5 Crash Location

Once the crash location was selected, separate simulations were conducted in Vissim 8.0 for each scenario and the results were analyzed. The crash blocked the right-most lane of the freeway. Partial vehicle routes were used to model the lane blockage. This prevents vehicles from using the segment of the lane that is closed for the duration of a crash. The length and location of the partial vehicle route can be adjusted by the analyst. This network element works similar to a static vehicle route function in Vissim. However, partial vehicle routes are used for changes that will be active only for a specific segment and lanes and can be also set to be active for a specific period of time during the simulation. Vehicles are automatically assigned to their original static vehicle routes after they leave a partial vehicle route (PTV, 2015). If using dynamic traffic assignment, dynamic routing decisions could be used. Rubbernecking was modeled using Reduced Speed Areas which were active during the crash. The Reduced Speed Areas extended 500 ft from the lane closure location with a desired speed of 20 mph as recommended in Chou and Miller-Hooks (2011).

Diversion of vehicles to alternate routes was not considered in this study since a network was not modeled and the collection of such data was outside the scope of this project. However, diversionary behavior of vehicles is expected to impact resilience. If this information is available,

the analyst should consider modeling diversionary behavior. The impact will be captured in the resilience analysis presented in this study.

4. Results

This section presents a discussion of the operational performance and the resilience-based analysis. The analysis focused on measuring resilience to demonstrate how practitioners and stakeholders can incorporate it in their decision-making process. The analysis was conducted at the segment level and the network level.

The segment-level analysis provided an understanding of the operations along the freeway for the different scenarios analyzed in this study. This is important for localized strategies to build resilience along the corridor. The network-level analysis provided an overview of the performance of the system as a whole. Although a network was not analyzed in this study, considering this measures are important to capture the overall impact. The following subsections of this study describe the results obtained for the segment-level analysis followed by a description of the results for the network-level analysis.

4.1 Segment-Level Analysis

Segment travel times and travel speeds were used for this analysis. These are common measures that have been found in transportation resilience-related research and traffic studies. Eight travel time segments along the freeway were created to collect travel times and derive travel speeds. These segments are shown in Figure 6. It can be seen in the figure that the crash occurred in travel time segment 6. Segments 1 through 5 were located upstream of the crash location and segments 7 and 8 were located downstream of the crash.

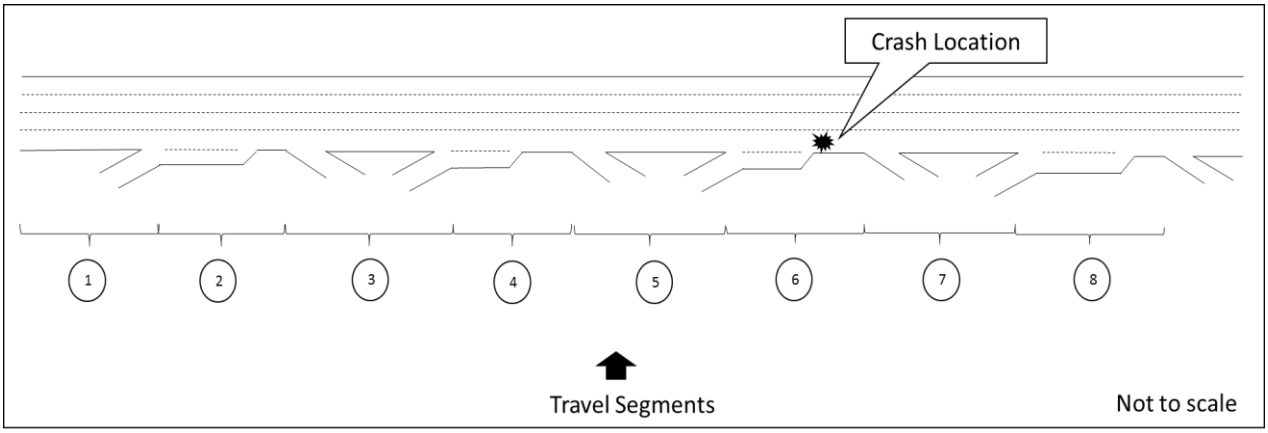

Figure 6 Travel Segments Created in Vissim

Travel time was collected at 15-minute intervals for the 24-hour simulation period and averaged over 10 simulation runs of different random seeds. The following subsections discuss in detail the results for travel times and speeds.

4.1.1 Travel Times

Figure 7 shows the travel time results for travel time segment 2. The figure illustrates the results right before, during, and after the lane closure for the scenarios evaluated in this study. Vertical lines were added to the figure to illustrate the crash start time and end time. Travel times for the no crash scenarios were also plotted and served as the baseline scenarios.

It can be seen from the figure that travel times for both crash scenarios increased compared to the corresponding base condition (no crash). Higher travel times were observed for the crash scenario without ramp metering (Scenario 3). Maximum travel time observed for that scenario was 5 minutes and 12 seconds which was an increase of approximately 3 minutes and 37 seconds compared to the no crash and no ramp metering (Scenario 1). For the crash scenario with ramp metering (Scenario 4), travel times peaked at 4 minutes and 42 seconds and started to decrease slightly after. This could be because the ramp meter was metering the demand from the ramps. The increase in travel time compared to the no crash scenario with ramp metering (Scenario 2) was approximately 4 minutes. The difference between Scenarios 2 and 4 was slightly higher than that for Scenarios 1 and 3 because the network was not congested in the no crash condition (Scenario 2).

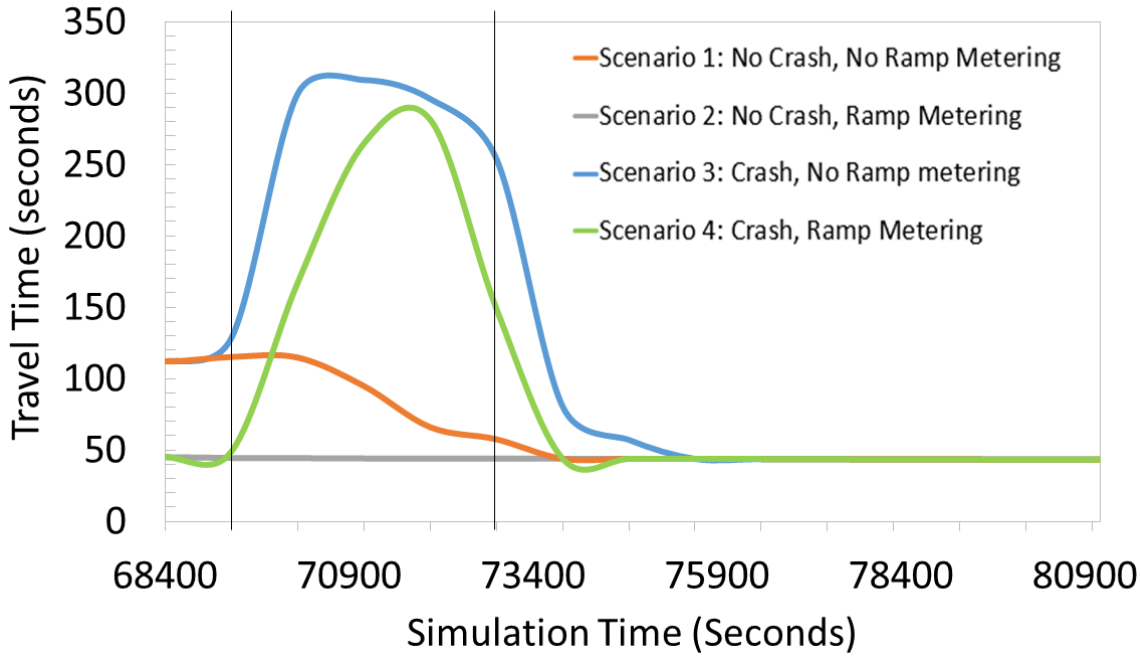

Figure 7 Travel Time Results

4.1.2 Travel Speeds

Figure 8 shows the travel speed results for study segment 2. The figure illustrates the results right before, during, and after the lane closure time for the scenarios evaluated in this

study. Vertical lines were added to the figure to illustrate the crash start time and end time. Travel speeds for the no crash scenarios were also plotted and served as the baseline scenarios.

Based on the results, travel speeds decreased with the crash compared to the corresponding base condition (no crash). Sometime after the crash was cleared, travel speeds started to increase and approached the travel speeds in the corresponding base scenario (no crash). Therefore indicating recovery. The minimum travel speed observed was 9.2 mph for the crash scenario without ramp metering (Scenario 3) which represented a speed drop of about 33.8 mph compared to the no crash scenario without ramp metering (Scenario 1). The minimum speed observed for the crash scenario with ramp metering (Scenario 4) was 10.2 mph which was a drop of 55.8 mph compared to the no crash scenario with ramp metering (Scenario 2). Similar to what was observed in the travel time results, the performance loss in the crash scenario with ramp metering compared to the no crash scenario was higher than that for the scenario without ramp metering. This is because the no crash scenario without ramp metering was operating at lower speeds. With the active ramp metering, the speeds were close to free-flow in the base scenario with no crash (Scenario2). However, recovery times should also be considered in the analysis.

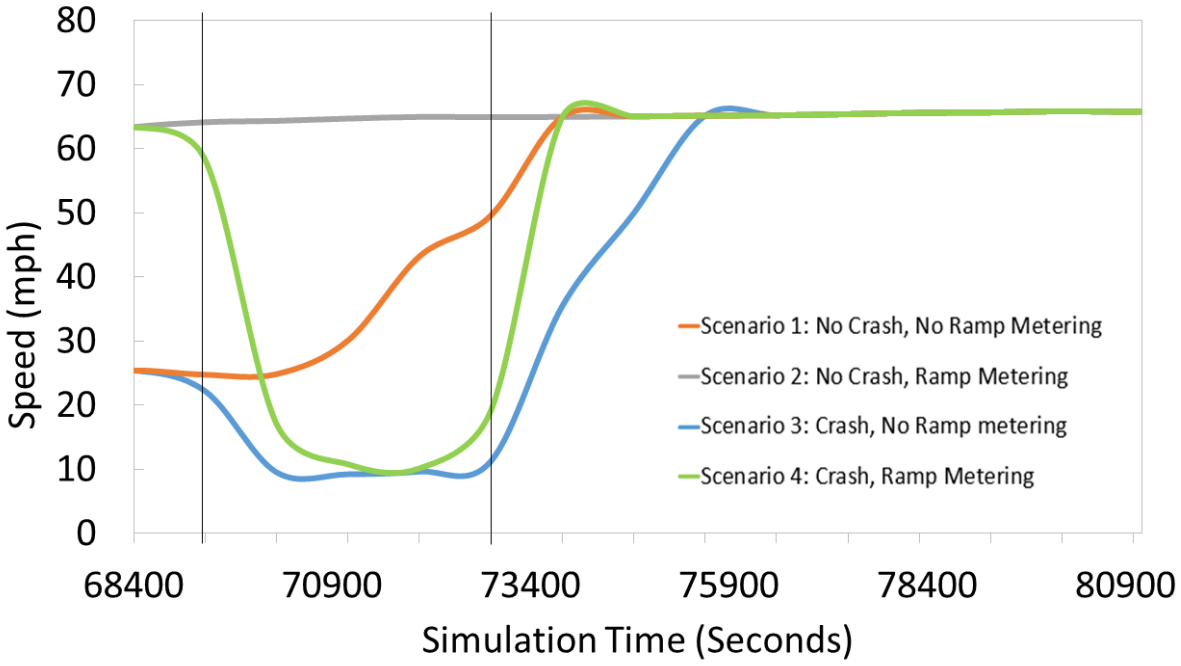

Figure 8 Travel Speed Results

Recovery times were computed for the crash scenarios. In this study, recovery was based on the time it took for the travel time segment to return to normal conditions after the lane blockage was removed. *Table 1* summarizes the recovery times for each of the crash scenarios. Based on the travel time and speed results, the segment recovered within 15 minutes after the crash when the ramp metering was active (Scenario 4). It took an additional 30 minutes for the segment to recover without the ramp metering (Scenario3).

Table 1 Summary of Recovery Times

Parameter	Scenario 1: No Crash, No Ramp Meter	Scenario 2: No Crash, Ramp Meter	Scenario 3: Crash, No Ramp Meter	Scenario 4: Crash, Ramp Meter
Travel Time	-	-	~45 minutes	~15 minutes
Travel Speed	-	-	~45 minutes	~15 minutes

4.1.3 Speed Heat Maps

To illustrate the speeds over time and space, speed heat maps were created for the freeway links as shown in Figure 9. This figure illustrates the heat maps for each of the scenarios studied. The columns represent the simulation time (15-minutes intervals) right before, during and, after the crash. The rows represent each of the link segments starting from the first segment at the bottom and the last segment at the top in the northbound direction. Therefore, traffic flows from bottom to top.

Overall, the heat maps illustrate that the freeway performed poorly for the no crash scenario without ramp metering (Scenario 1) as seen in Figure 9 (a) compared to the scenario with ramp metering (Scenario 2) in Figure 9 (b). Some bottlenecks were observed in Scenario 2 with speeds of 15 mph or less. However, overall average speeds for the entire period shown was 54.6 mph and 45.2 mph with ramp metering and without ramp metering, respectively.

Additional stress on the system due to a lane blockage on link 6 created lower speeds in both crash scenarios compared to their corresponding no crash scenarios (Scenario 1 vs. Scenario 3 and Scenario 2 vs. Scenario 4). The crash created a bottleneck on link 6 which propagated all the way to the beginning of the network (link 102) in the crash scenario without the ramp metering (Scenario 3) as shown in Figure 9 (c). In the crash scenario with ramp metering (Scenario 4) the impact did not propagate as far as shown in Figure 9 (d). Downstream of the crash location, close to free-flowing conditions were observed in both crash scenarios. This was expected as the crash was holding the traffic and having a metering effect on the flow.

Regarding the temporal effect of the crash, the figures show that link speeds after the crash was cleared were increasing faster in the scenario with the ramp metering while some links were still recovering in the scenario without ramp metering for the same time periods. Link 102 which was the farthest link from the crash location was the last to recover in the crash scenario without ramp metering (Scenario 3). Average speeds of all links during the crash were 29.19 mph and 24.6 mph when the ramp meter was active (Scenario 4) and when it was inactive (Scenario 3), respectively.

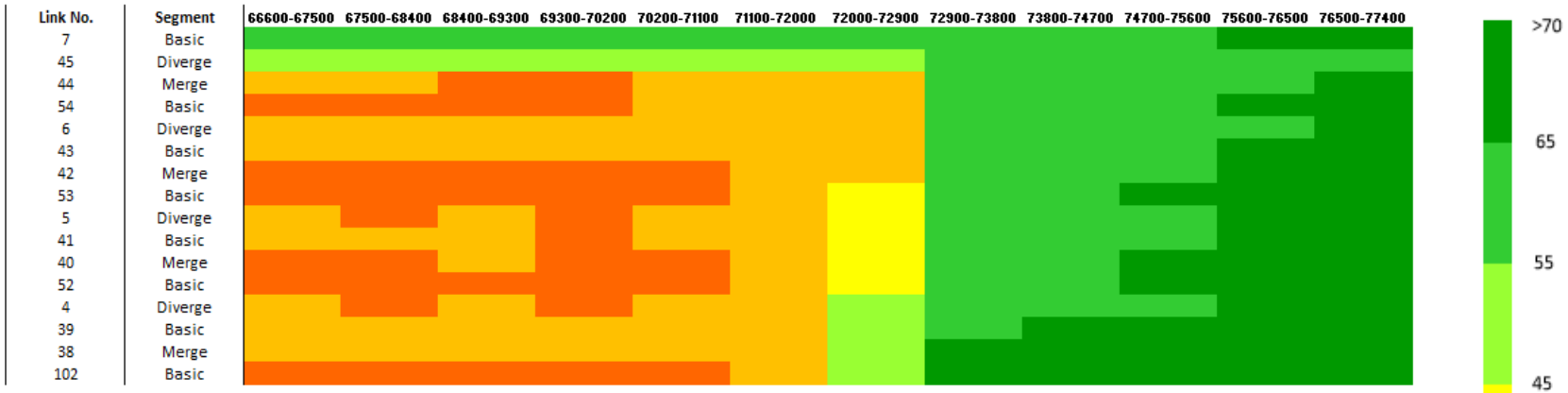
Link No.
Segment
66600-67500
67500-68400
68400-69300
69300-70200
70200-71100
71100-72000
72000-72900
72900-73800
73800-74700
74700-75600
75600-76500
76500-77400
7 Basic
45 Diverge
44 Merge
54 Basic
6 Diverge
43 Basic
42 Merge
53 Basic
5 Diverge
41 Basic
40 Merge
52 Basic
4 Diverge
39 Basic
38 Merge
102 Basic
>70
65
55
45
35
25
15
0

(a)

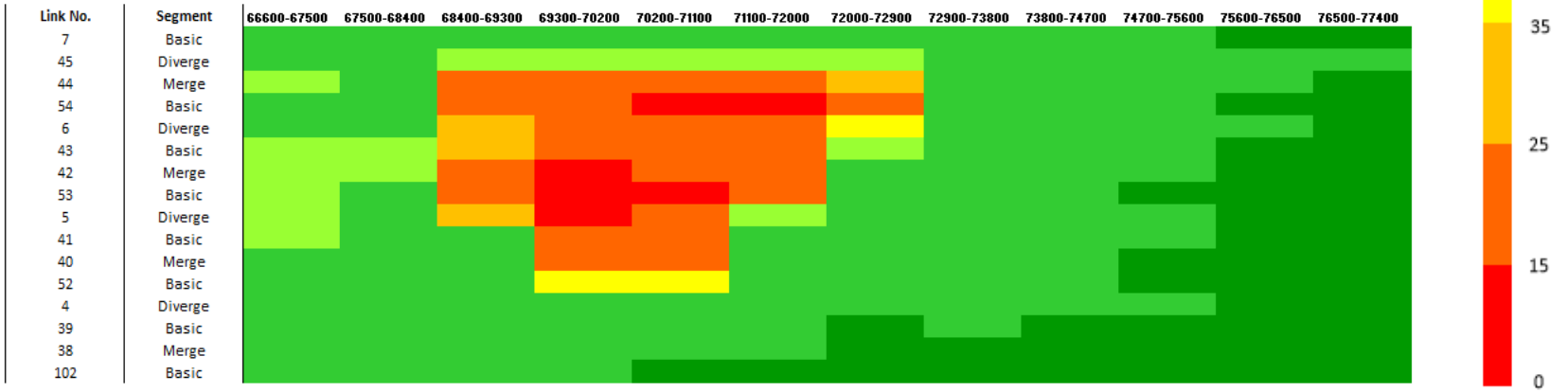
Link No.
Segment
66600-67500
67500-68400
68400-69300
69300-70200
70200-71100
71100-72000
72000-72900
72900-73800
73800-74700
74700-75600
75600-76500
76500-77400
7 Basic
45 Diverge
44 Merge
54 Basic
6 Diverge
43 Basic
42 Merge
53 Basic
5 Diverge
41 Basic
40 Merge
52 Basic
4 Diverge
39 Basic
38 Merge
102 Basic

(b)

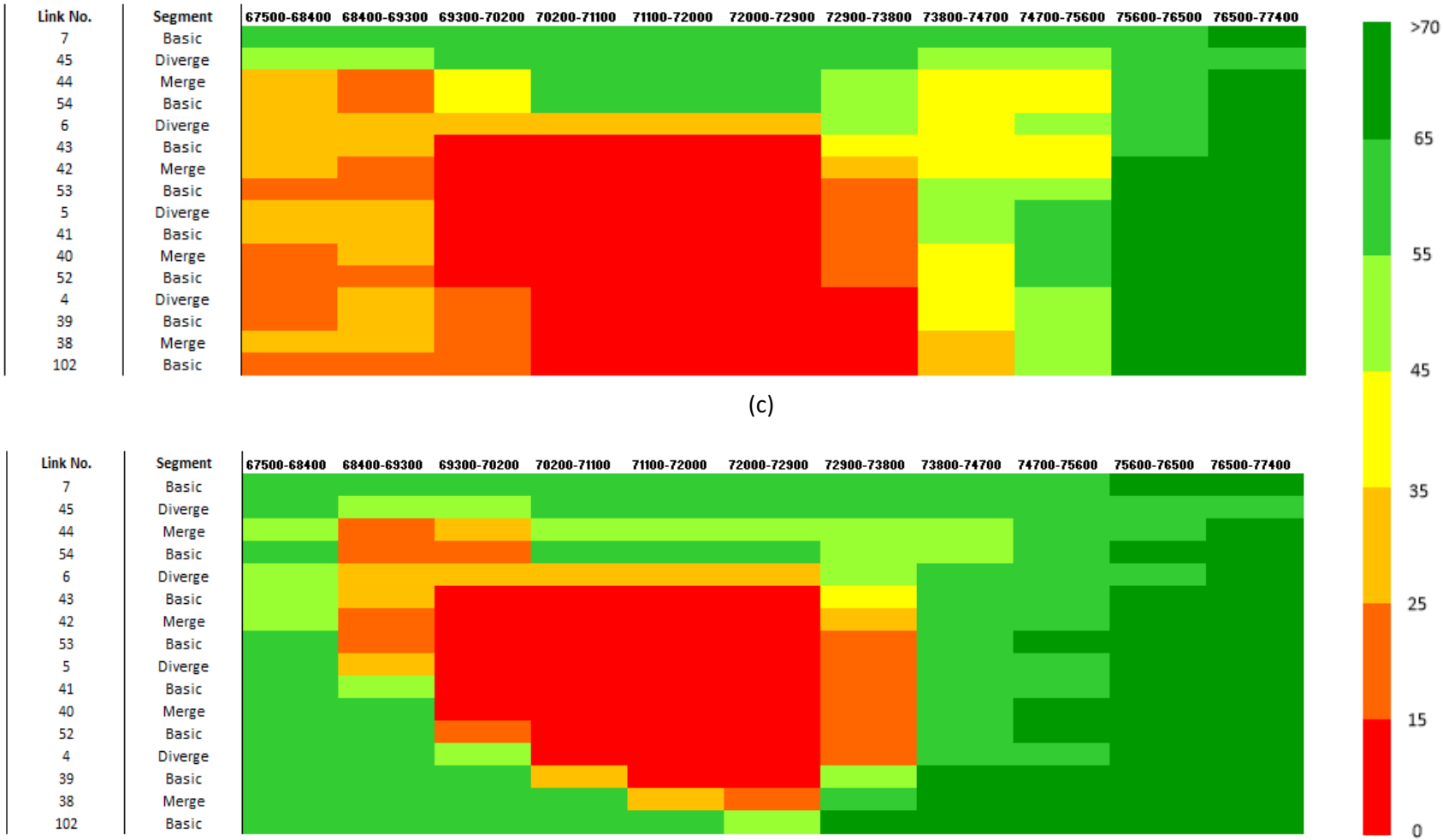

(c)

(d)

Figure 9 Speed Heat Maps for (a) Scenario 1 (no crash, no ramp metering), (b) Scenario 2 (no crash, ramp metering), (c) Scenario 3 (crash, no ramp metering), and (d) Scenario 4 (crash, ramp metering)

4.1.4 Link Performance Indicator for Resilience (LPIR)

A separate analysis was conducted to quantify the resilience of freeway segments using the LPRI value derived by Calvert & Snelder (2017). An LPIR value lower or equal to 1 indicates that a road section is able to resist a significant drop in level-of-service and/or recover quickly from a significant drop in performance.

Table 2 summarizes the LPIR values for each segment in each scenario. The table shows that the LPIR values for the no crash scenarios were less than 1 except with a few segments that had a value of 1.1. This shows that the system was able to resist the regular traffic flows for that period without a crash.

In the presence of a disruption on traffic flow from a temporary lane blockage, some road segments were not able to resist and/or recover quickly in the scenario with no ramp metering (Scenario 3). LPIR values were between 0.5 and 1.5 for that scenario. All the links upstream of the crash location had LPIR values larger than 1. External factors, in this case ramp metering, helped the segments as observed with LPRI values lower than 1 or close to 1 in Scenario 4. LPIR values were between 0.4 and 1.1 for that scenario. It is important to note that a LPIR value larger than 1 does not always means that the segment is non-resilient (Calvert and Snelder, 2017).

Table 2 Summary of LPIR Values for each Segment

Link No.	No. Lane	LPRI Value			
		Scenario 1: No Crash, No Ramp Metering	**Scenario 2: No Crash, Ramp Metering**	**Scenario 3: Crash, No Ramp Metering**	**Scenario 4: Crash, Ramp Metering**
7	4	0.5	0.5	0.5	0.4
45	4	0.7	0.6	0.7	0.6
44	5	0.9	0.7	0.9	0.6
54	4	0.9	0.7	0.8	0.5
6*	4	1.0	0.8	1.0	0.7
43	4	0.8	0.6	1.0	0.8
42	5	0.9	0.7	1.2	0.9
53	4	0.9	0.6	1.2	0.9
5	4	1.1	0.7	1.4	1.1
41	4	0.8	0.5	1.1	0.8
40	5	0.9	0.5	1.2	0.8
52	4	0.9	0.4	1.2	0.8
4	4	1.1	0.5	1.5	1.0
39	4	0.8	0.4	1.1	0.6
38	5	0.8	0.4	1.2	0.6
102	4	0.9	0.4	1.2	0.4

*Crash location

4.2 Network-Level Analysis

Network performance results from Vissim were analyzed. More specifically, the authors assessed Vehicle Hours Traveled (VHT) and Vehicle Hours of Delay (VHD). Vehicle Miles Traveled (VMT) is critical for comparing the additional miles driven by vehicles taking alternate routes. This is useful when considering route detours. In this study, however, detours were not considered.

Table 3 summarizes VHT and VHD results for each scenario. As expected, the analysis showed that both VHT and VHD were higher with a crash compared to having no disruptions. The highest VHT and VHD were observed for the crash scenario without ramp metering (Scenario 3) which is consistent with the segment-level results. However, this study only considered a freeway segment which limited the ability to capture the impact on a network.

Table 3 Network-Wide Results for all Scenarios

Network Parameter	Scenario 1: No Crash, No Ramp Metering	Scenario 2: No Crash, Ramp Metering	Scenario 3: Crash, No Ramp Metering	Scenario 4: Crash, Ramp Metering
Vehicle Hours Traveled (hr)	12,261	10,263	13,235	10,797
Vehicle Hours of Delay (hr)	4,454	2,452	5,429	2,986

5. Conclusions

This study demonstrated the use of resilience methods and metrics found in the literature in the analysis of a traffic simulation that modeled a lane blockage due to a crash. Ramp metering was modeled and considered as a traffic operation strategy to increase resilience. A crash scenario without ramp metering was also assessed and considered as a "Do-Nothing" or "No-Build" scenario typically used in the alternative design process in transportation projects. For this study, travel speeds and travel times were selected for the analysis to measure resilience at the segment level. In addition, the Link Performance Indicator for Resilience (LIPR) score developed by Calvert & Snelder (2017) was evaluated. A network-level analysis was also conducted using network performance measures: vehicle hours traveled (VHT) and vehicle hours of delay (VHD).

The results showed that the resilience metrics and methods implemented in this study seemed to have captured the resilience of the freeway using simulation. The results of the analysis also showed that active ramp metering improved the resilience of the freeway based on all of the methods and metrics considered in this study. However, more research may still be needed to understand the resilience metrics and methods that can be implemented in different type of scenarios so that guidance can be provided to practitioners.

Some assumptions were made in this study which created limitations and opportunities to expand in future research. The first limitation was that this study only modeled a freeway segment and did not include a network. Modeling a network accounts for conditions such as

queue spillbacks onto arterial roads. The second limitation was that the study did not consider different crash scenarios with different crash clearance times, crash locations, and time of day. Faster clearance times can reduce the impact on the network. Similarly, a crash occurring during a time of day with higher demand can impact the results. The third limitation of this study was that diversionary behavior from the crash was not considered which can alleviate congestion on the freeway and also result in congested arterials and minor streets because they do not have enough capacity to carry the increased demand.

6. References

1. Attoh-Okine, N. O., Cooper, A. T., & Mensah, S. A. (2009). Formulation of resilience index of urban infrastructure using belief functions. *IEEE Systems Journal*, *3*(2), 147–153. https://doi.org/10.1109/JSYST.2009.2019148.

2. Balal, E., Valdez, G., Miramontes, J., & Cheu, R. L. (2019). Comparative evaluation of measures for urban highway network resilience due to traffic incidents. *International Journal of Transportation Science and Technology*, *8*(3), 304–317. https://doi.org/10.1016/j.ijtst.2019.05.001

3. Berdica, K. (2002). An introduction to road vulnerability: What has been done, is done and should be done. *Transport Policy*, *9*(2), 117–127. https://doi.org/10.1016/S0967-070X(02)00011-2

4. Blackmore, J. M., & Plant, R. A. J. (2008). Risk and resilience to enhance sustainability with application to urban water systems. *Journal of Water Resources Planning and Management*, *134*(3), 224–233. https://doi.org/10.1061/(ASCE)0733-9496(2008)134:3(224)

5. Bozza, A., Asprone, D., & Fabbrocino, F. (2017). Urban resilience: A civil engineering perspective. *Sustainability (Switzerland)*, *9*(1), 1–17. https://doi.org/10.3390/su9010103

6. Bruneau, M., Chang, S. E., Eguchi, R. T., Lee, G. C., O'Rourke, T. D., Reinhorn, A. M., Shinozuka, M., Tierney, K., Wallace, W. A., & Von Winterfeldt, D. (2003). A Framework to Quantitatively Assess and Enhance the Seismic Resilience of Communities. *Earthquake Spectra*, *19*(4), 733–752. https://doi.org/10.1193/1.1623497

7. Bruneau, M., & Reinhorn, A. (2007). Exploring the concept of seismic resilience for acute care facilities. *Earthquake Spectra*, *23*(1), 41–62. https://doi.org/10.1193/1.2431396

8. California Department of Transportation, Retrieved from http://pems.dot.ca.gov

9. Calvert, S. C., & Snelder, M. (2018). A methodology for road traffic resilience analysis and review of related concepts. *Transportmetrica A: Transport Science*, *14*(1–2), 130–154. https://doi.org/10.1080/23249935.2017.1363315

10. Chen, L., & Miller-Hooks, E. (2012). Resilience: An indicator of recovery capability in intermodal freight transport. *Transportation Science*, *46*(1), 109–123. https://doi.org/10.1287/trsc.1110.0376

11. Chou, C. S., & Miller-Hooks, E. (2011). Exploiting the capacity of managed lanes in diverting traffic around an incident. *Transportation Research Record*, *2229*, 75–84. https://doi.org/10.3141/2229-09

12. Cox, Andrew, Fynnwin Prager, & Adam Rose. 2011. "Transportation Security and the Role of Resilience: A Foundation for Operational Metrics." *Transport Policy* 18 (2): 307–317.

13. Crucitti, P., Latora, V., & Marchiori, M. (2004). Model for cascading failures in complex networks. *Physical Review E - Statistical Physics, Plasmas, Fluids, and Related Interdisciplinary Topics*, *69*(4), 4. https://doi.org/10.1103/PhysRevE.69.045104

14. D'Lima, M., & Medda, F. (2015). A new measure of resilience: An application to the London Underground. *Transportation Research Part A: Policy and Practice*, *81*, 35–46. https://doi.org/10.1016/j.tra.2015.05.017

15. Donovan, B., & Work, D. B. (2017). Empirically quantifying city-scale transportation system resilience to extreme events. *Transportation Research Part C: Emerging Technologies*, *79*, 333–346. https://doi.org/10.1016/j.trc.2017.03.002

16. Dowling, R., Skabardonis, A., & Alexiadis, V. (2004). Traffic Analysis Toolbox Volume III: Guidelines for Applying Traffic Microsimulation Software. FHWA-HRT-04-040

17. Farhadi, N., Parr, S. A., Mitchell, K. N., & Wolshon, B. (2016). Use of nationwide automatic identification system data to quantify resiliency of marine transportation systems. *Transportation Research Record*, *2549*(January), 9–18. https://doi.org/10.3141/2549-02

18. FHWA. Transportation System Resilience to Extreme Weather and Climate Change. Federal Highway Administration. November (2015). http://www.ops. fhwa.dot.gov/publications/fhwahop15024/fhwahop15024.pdf. Accessed June 9, 2016.

19. FHWA. Fixing America's Surface Transportation Act or "FAST Act" Retrieved from https://www.fhwa.dot.gov/fastact/summary.cfm Accessed on August 27, 2020.

20. Gay, L. F., & Sinha, S. K. (2013). Resilience of civil infrastructure systems: Literature review for improved asset management. *International Journal of Critical Infrastructures*, *9*(4), 330–350. https://doi.org/10.1504/IJCIS.2013.058172

21. Healy, K. (2014). *Measuring the resilience of transport infrastructure February 2014* (Issue February).

22. Henry, D., & Emmanuel Ramirez-Marquez, J. (2012). Generic metrics and quantitative approaches for system resilience as a function of time. *Reliability Engineering and System Safety*, *99*, 114–122. https://doi.org/10.1016/j.ress.2011.09.002

23. Holling, C. S. (1973). Resilience and Stability of Ecological Systems. *Annual Review of Ecology and Systematics*, *4*, 1–23.

24. Holme, P., Kim, B. J., Yoon, C. N., & Han, S. K. (2002). Attack vulnerability of complex networks. *Physical Review E - Statistical Physics, Plasmas, Fluids, and Related Interdisciplinary Topics*, *65*(5), 14. https://doi.org/10.1103/PhysRevE.65.056109

25. Ip, W. H., & Wang, D. (2011). Resilience and friability of transportation networks: Evaluation, analysis and optimization. *IEEE Systems Journal*, *5*(2), 189–198. https://doi.org/10.1109/JSYST.2010.2096670

26. Kim, S., & Yeo, H. (2016). A Flow-based Vulnerability Measure for the Resilience of Urban Road Network. *Procedia - Social and Behavioral Sciences*, *218*, 13–23.

https://doi.org/10.1016/j.sbspro.2016.04.006

27. Li, Y., & Lence, B. J. (2007). Estimating resilience for water resources systems. *Water Resources Research*, *43*(7), 1–11. https://doi.org/10.1029/2006WR005636

28. McManus, S., Seville, E., Vargo, J., & Brunsdon, D. (2008). Facilitated process for improving organizational resilience. *Natural Hazards Review*, *9*(2), 81–90. https://doi.org/10.1061/(ASCE)1527-6988(2008)9:2(81)

29. Murray-Tuite, P. M. (2006). A comparison of transportation network resilience under simulated system optimum and user equilibrium conditions. *Proceedings - Winter Simulation Conference*, 1398–1405. https://doi.org/10.1109/WSC.2006.323240

30. Najjar, W., & Gaudiot, J. L. (1990). Network Resilience: A Measure of Network Fault Tolerance. *IEEE Transactions on Computers*, *39*(2), 174–181. https://doi.org/10.1109/12.45203

31. Nicholson, C. D., Barker, K., & Ramirez-Marquez, J. E. (2016). Flow-based vulnerability measures for network component importance: Experimentation with preparedness planning. *Reliability Engineering and System Safety*, *145*, 62–73. https://doi.org/10.1016/j.ress.2015.08.014

32. PTV User Manual, 2015.

33. Reggiani, A., De Graaff, T., & Nijkamp, P. (2002). Resilience: An Evolutionary Approach to Spatial Economic Systems. *Networks and Spatial Economics*, *2*(2), 211–229. https://doi.org/10.1023/A:1015377515690

34. Reggiani, A., Nijkamp, P., & Lanzi, D. (2015). Transport resilience and vulnerability: The role of connectivity. *Transportation Research Part A: Policy and Practice*, *81*, 4–15. https://doi.org/10.1016/j.tra.2014.12.012

35. Scott, D. M., Novak, D. C., Aultman-Hall, L., & Guo, F. (2006). Network Robustness Index: A new method for identifying critical links and evaluating the performance of transportation networks. *Journal of Transport Geography*, *14*(3), 215–227. https://doi.org/10.1016/j.jtrangeo.2005.10.003

37. Shojaat, S., Geistefeldt, J., Parr, S. A., Escobar, L., & Wolshon, B (2018). Defining Freeway Design Capacity Based on Stochastic Observations. *Transportation Research Record: Journal of the Transportation Research Board*. 2672: 131–141. https://doi.org/10.1177/0361198118784401

38. Shojaat, S (2017). Sustained Flow Index: A Stochastic Measure of Freeway Performance. LSU Doctoral Dissertations. 4170. https://digitalcommons.lsu.edu/gradschool_dissertations/4170

37. Somers, S. (2009). Measuring resilience potential: An adaptive strategy for organizational crisis planning. *Journal of Contingencies and Crisis Management*, *17*(1), 12–23. https://doi.org/10.1111/j.1468-5973.2009.00558.x

38. Sullivan, J. L., Novak, D. C., Aultman-Hall, L., & Scott, D. M. (2010). Identifying critical road

segments and measuring system-wide robustness in transportation networks with isolating links: A link-based capacity-reduction approach. *Transportation Research Part A: Policy and Practice*, *44*(5), 323–336. https://doi.org/10.1016/j.tra.2010.02.003

39. Trivedi, K. S., Kim, D. S., & Ghosh, R. (2009). Resilience in computer systems and networks. *IEEE/ACM International Conference on Computer-Aided Design, Digest of Technical Papers, ICCAD*, 74–77. https://doi.org/10.1145/1687399.1687415

40. Vugrin, E. D., Warren, D. E., Ehlen, M. A., & Camphouse, R. C. (2010). *A Framework for Assessing the Resilience of Infrastructure and Economic Systems*. Springer-Verlag Berlin Heidelberg.

41. Zhang, W., & Wang, N. (2016). Resilience-based risk mitigation for road networks. *Structural Safety*, *62*(May 2018), 57–65. https://doi.org/10.1016/j.strusafe.2016.06.003

42. Zhu, Y., Ozbay, K., Xie, K., & Yang, H. (2016). Using big data to study resilience of taxi and subway trips for Hurricanes Sandy and Irene. *Transportation Research Record*, *2599*(December), 70–80. https://doi.org/10.3141/2599-09